

RESEARCH ARTICLE



WILEY

2-step process for 5.4% CuGaSe₂ solar cell using fluorine doped tin oxide transparent back contacts

Angélica Thomere¹ | Marcel Placidi^{1,3} | Maxim Guc¹ | Kunal Tiwari¹ | Robert Fonoll-Rubio¹ | Victor Izquierdo-Roca¹ | Alejandro Perez-Rodriguez^{1,2} | Zacharie Jehl Li-Kao³

¹IREC Institut de Recerca en Energia de Catalunya, Jardins de les Dones de Negre 1, 2^a pl, Sant Adrià del Besòs, Barcelona, 08930, Spain

²IN2UB, Departament d'Enginyeria Electrònica i Biomèdica, Universitat de Barcelona, Carrer de Martí i Franquès 1, Barcelona, 08028, Spain

³Departament d'Enginyeria Electrònica & Barcelona Center for Multiscale Science & Engineering, Universitat Politècnica de Catalunya, Av Eduard Maristany 10-14, Barcelona, 08019, Spain

Correspondence

Angélica Thomere and Marcel Placidi, IREC Institut de Recerca en Energia de Catalunya, Jardins de les Dones de Negre 1, 2^a pl., Sant Adrià del Besòs 08930, Barcelona, Spain.

Email: athomere@irec.cat and marcel.placidi@upc.edu

Funding information

Ministerio de Ciencia e Innovación; R+D+i Cell2Win project, Grant/Award Number: PID 2019-104372RB-C31; Generalitat de Catalunya, Grant/Award Number: 2017 SGR 862; Ramón y Cajal, Grant/Award Number: RYC-2017-23758; Juan de la Cierva, Grant/Award Number: IJC2018-038199-I

Abstract

As single-junction solar cells are approaching theoretical limits, multijunction solar cells are becoming increasingly relevant, and low-cost wider bandgap light harvesters in tandem with silicon are the next frontier in thin film photovoltaic research. Cu-based chalcogenide compounds have achieved great success as standard absorbers, but performance for bandgaps above 1.5 eV is still lacking. Additionally, the use of transparent back contacts remains challenging for this class of materials. In this work, we report on the fabrication of wide bandgap CuGaSe₂ absorbers by a combination of metallic sputtering and reactive thermal annealing grown on transparent fluorine-doped tin oxide-coated glass substrate. The annealing temperature is carefully tuned in regard to material and photovoltaic device properties. The introduction of an ultrathin Mo interlayer at the CuGaSe₂/back interface favors a higher contact's ohmicity and results in an important improvement of all figures of merit. A record conversion efficiency of 5.4% is obtained, which is the highest value reported for this class of absorber on transparent back contact. Fundamental material characterization of the as-grown CuGaSe₂ films reveals a better homogeneity in Cu distribution throughout the absorber's thickness when using a Mo interlayer, along with an enhanced crystalline quality. The sub-bandgap transparency of the final device remains perfectible, and improvement pathways are proposed using transfer matrix-based optical modeling, suggesting to use more specular interfaces to enhance optical transmission.

KEYWORDS

CIGS solar cell, transparent back contact, wide bandgap

1 | INTRODUCTION

Single-junction photovoltaic (PV) devices have reached a level of maturity, permitting the realization of solar modules with efficiencies

well above 20% at a forecasted cost below 0.30€/Wp⁻¹ by the year 2020.¹ Whereas crystalline silicon (c-Si) remains by far the dominant technology, the advent of thin film technologies above 20% efficiency, including perovskite and Cu (In,Ga)(S,Se)₂ (CIGS) absorbers, brings

This is an open access article under the terms of the [Creative Commons Attribution-NonCommercial-NoDerivs](https://creativecommons.org/licenses/by-nc-nd/4.0/) License, which permits use and distribution in any medium, provided the original work is properly cited, the use is non-commercial and no modifications or adaptations are made.

© 2022 The Authors. Progress in Photovoltaics: Research and Applications published by John Wiley & Sons Ltd.

new opportunities for the field in terms of emerging applications, such as building-integrated photovoltaics (BIPV) and Internet of Things (IoT). The tunability of these materials' bandgap permits their utilization as top cell in tandem with a c-Si bottom cell, and it appears that affordable multijunction designs represent the future of large-scale PV installations. In that context, chalcopyrite CIGS solar cells are an attractive option as their bandgap can be tuned in a wide range by controlling the cations (In and Ga) and/or anions (S and Se) ratios. However, although the record conversion efficiency is 23.35% for a mixed compound Cu(In,Ga)(Se,S)₂,² increasing the bandgap to values above 1.6 eV often means pursuing high Ga content materials, and the Ga-related defects have proven markedly more detrimental than In-related defects.^{3,4} Pure Ga CuGaSe₂ (CGSe) has an ideal 1.68 eV bandgap for tandem application,⁵ and the highest reported efficiency for this material is 11.9%, utilizing an opaque Mo back electrode.⁶ However, exploring this bandgap range while using opaque metallic back contacts can appear pointless as the optical transmission is lost in the back electrode. The realization of wide bandgap chalcopyrite absorbers on transparent substrates remains challenging with the highest reported efficiency value for CGSe-based cells on an indium tin oxide (ITO) substrate being 5%⁷ and 4.3% on fluorine-doped tin oxide (FTO).^{8,9} If this class of material is to become a serious contender for tandem application, a breakthrough in terms of performance is therefore needed in the upcoming years.

The fabrication of standard, narrow bandgap CIGSe solar cells on transparent substrates has been pioneered by Nakada *et al.* throughout the 2000s,^{10,11} using both ITO and FTO as back contacting electrodes; it was however reported by the same group that ZnO:Al, another commonly used transparent conducting oxide (TCO), did not lead to the formation of an ohmic contact with a chalcopyrite absorber. It was found that the insertion of an ultrathin Mo layer at the absorber/TCO interface markedly improved the solar cells' performance, which can be ascribed to the formation of a MoSe₂ interlayer acting as hole-selective material. Our group recently observed a similar trend working on lower band gap CIGS devices,¹² as well as with a wider bandgap (1.4 eV) CIGSe material with a 68% Ga content,¹³ which seems to indicate that observations made on the low Ga content are to some extent transferrable to the higher Ga counterpart despite the modified band profile.

In the present work, we aim at fabricating pure Ga, wide bandgap CGSe-based solar cells on transparent FTO substrate for a potential application as semitransparent devices or to tandem devices in combination with c-Si or with a well-established narrow bandgap thin film material, such as CIGSe $E_g = 1.1$ eV. Unlike the previous record for CGSe solar cell, which relied on co-evaporated films,⁷ the CGSe absorbers are fabricated using a combination of metallic precursor deposition by direct current (DC) sputtering and reactive thermal annealing In-Se atmosphere. This process is comparable to the one reported for the current CIGSe efficiency record,² albeit without sulfurization step nor Indium element, resulting in a much wider bandgap in the present case. In a first step, the FTO/CGSe interface is optimized, and the presence of an interfacial Mo is found instrumental in increasing the cells' performance, a result consistent with Nakada

et al.'s observation.¹⁰ It should be noted that Choi *et al.*⁷ did not include such Mo interlayer. In a second step, parameters of the annealing process are varied, and their individual influence is assessed. It nevertheless appears that while a high annealing temperature is preferable to improve the films' crystallinity, temperatures of 600°C degrade the devices, which are ascribed to a degradation of the back FTO electrode. The optical analysis of the fabricated devices indicates a total optical transmission of about 30% below the absorber's bandgap, an encouraging value for semitransparent applications yet still too limiting for a tandem application. Using transfer matrix-based optical modeling, we demonstrate that reducing the surface roughness is a possible pathway to markedly improve the optical transmission of CGSe solar cells. The record device presented here reaches an efficiency of 5.4% without antireflective coating, a value higher than the state of the art for this material fabricated on TCO transparent substrate.^{7,8}

2 | RESULTS AND DISCUSSION

2.1 | Back interface optimization

The importance of optimizing the back contact in chalcopyrite-based absorber for specific applications has previously been reported,^{10,14,15} though the natural occurrence of an ohmic back contact when working with Mo substrates has greatly streamlined the work in that regard when dealing with standard PV applications. In the present study, two important modifications are made as compared to standard CIGSe devices: a pure Ga wide bandgap CuGaSe₂ absorber and the use of a transparent FTO substrate. Hence, optimizing the ohmicity of the back interface becomes critical to achieve good conversion efficiencies.

As widely reported,^{16,17} the good quality of the Mo/CGSe interface is ascribed to the formation of a thin MoSe₂ layer, acting as a hole transport material. Alternative promising interlayers have been proposed,¹⁸ but MoSe₂ has so far the best proven track record for the fabrication of chalcopyrite absorbers on a TCO substrate.^{10,13} Whereas functioning CuGaSe₂ solar cell devices have previously been reported on a TCO substrate,⁶ the change in band profile as compared to narrower bandgap compounds and its subsequent influence on the back contact ohmicity is yet to be reported. In the first part of this work, we therefore compare the cases of CuGaSe₂ absorbers fabricated on bare FTO and FTO/Mo (15 nm), with the assumption that the latter case leads to a full selenization of the ultrathin Mo layer. In these experiments, no intentional Na doping has been performed, and the FTO is acting as a barrier preventing Na diffusion from the glass substrate.¹⁹

The results of the characterization by current-voltage analysis of both types of devices are presented Figure 1. The absorber for both sample series was grown in the same experimental run.

The peak voltages are similar in both cases, with a $V_{OC}^{max} \cong 650$ mV. This is expected when comparing two similar absorbers as the quasi-Fermi level splitting should be identical and could in this case be ascribed to a limitation at the p-n interface due to the cliff-like band alignment between CGSe and cadmium sulphide (CdS). The larger data spread for the bare FTO case may indicate a generally lower material

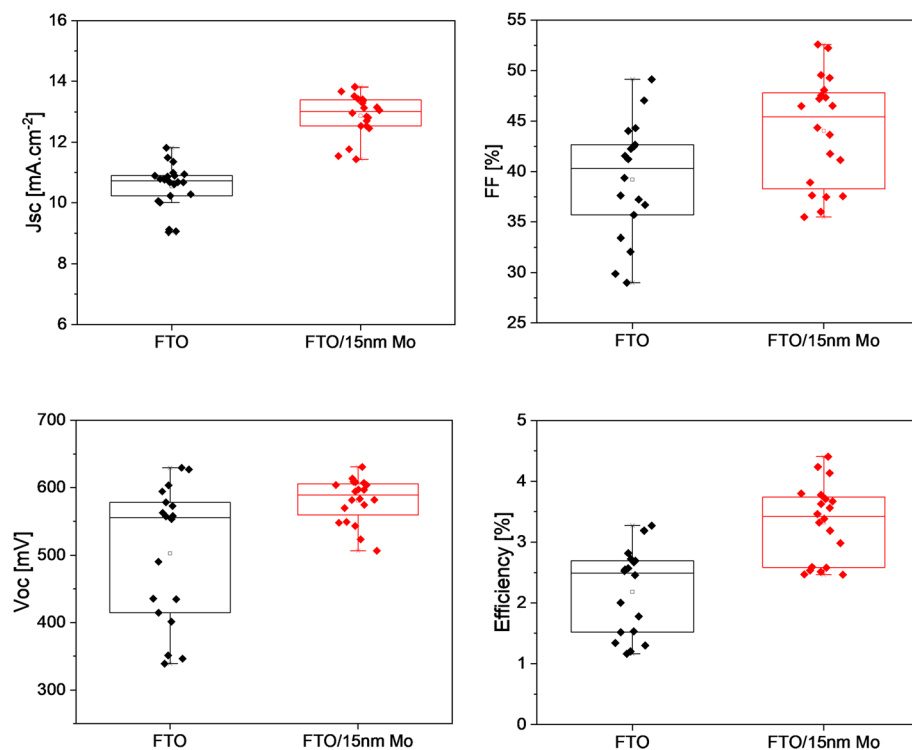


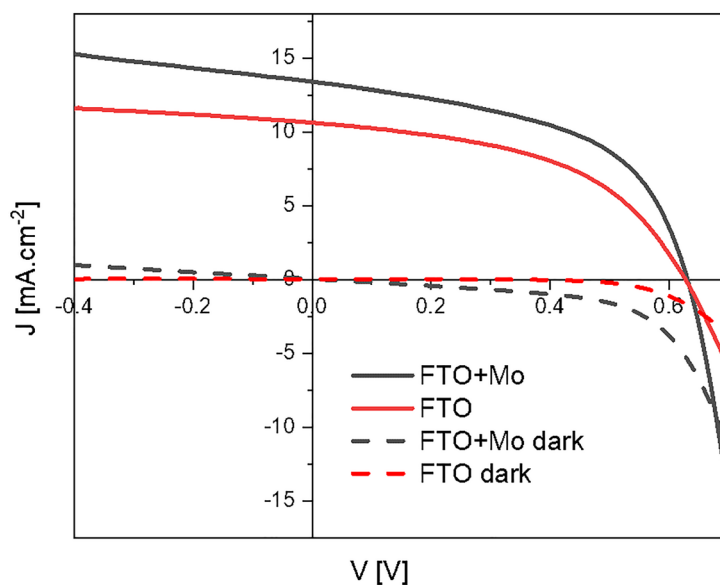
FIGURE 1 Photovoltaic parameters of the solar cells prepared with and without the interlayer of Mo

homogeneity with the possibility of phase segregation or locally poor material nucleation, strongly affecting the open-circuit voltage when present. Additionally, the density of short-circuit current data spread appears very similar between both configurations, with a $\Delta J_{sc} \approx 2.5 \text{ mA}\cdot\text{cm}^{-2}$; however, the overall values (peak and median) are significantly higher in the presence of an Mo interlayer, indicating that loss mechanisms occur when CGSe is fabricated on the bare FTO substrate. The study by Choi *et al.*⁷ indicates comparable results with an appreciable difference in the current density between CGSe absorbers grown on bare ITO and absorbers grown on a thick Mo electrode. The J-V curves and corresponding parameters of the highest efficiency cells in both series are reported Figure 2. The discrepancy in current density values between CGSe absorbers grown on FTO/Mo and bare FTO ($J_{sc} = 13.4 \text{ mA}\cdot\text{cm}^{-2}$ against $10.6 \text{ mA}\cdot\text{cm}^{-2}$ respectively) can be explained by different hypotheses; the most straightforward one would be that in the absence of MoSe_2 , acting as an electron reflector, back contact recombination becomes predominant and significantly reduces the current. However, this behavior is hardly supported by numerical modeling, as illustrated in the Supporting Information Figure S1, which shows the case of a CGSe solar modeled using Solar Cell Capacitance Simulator (SCAPS) with and without a back electron reflector. Considering an absorber thickness of 1600 nm as determined by X-ray fluorescence (XRF) analysis, a carrier diffusion length of 500 nm, and a realistic absorption profile with data from Paulson *et al.*,²⁰ the back contact is not expected to have an influence on the photogenerated carriers as those never diffuse to that point, and the calculated quantum efficiency between both cases is nearly similar. In that context, holes “extraction through the back contact is the only relevant parameter to consider. Another possibility consistent with the observed differences in the current values from the devices grown

on bare FTO and on FTO/Mo back contacts is related to bulk recombination, preventing photocarriers generated in the flat band region to properly diffuse toward the p-n interface. This interpretation, common in thin film based solar cells, will be later discussed in the context of External Quantum Efficiency analyses. Finally, the possible formation of a secondary phase at the absorber/back contact interface from the devices made on bare FTO back contacts may act as a barrier impairing holes’ extraction, thus partially reducing the current. This latter hypothesis is also consistent with the observation made when comparing the Fill Factor (FF) of both configurations in Figure 1 and Figure 2. Despite a similar data spread in both cases (Figure 1), possibly related to an inhomogeneity of the material independent from the back contact, the peak and median FF values are 5% higher in absolute in the presence of a Mo interlayer. Variations of the FF independently from the voltage are likely to be ascribed to resistive effects; in this case, series resistance, which beyond certain values, starts affecting the J_{sc} , as it is observed here, with R_s increasing from 4 to $157 \Omega\cdot\text{cm}^{-2}$ with and without interfacial Mo, respectively. The presence of this back interface barrier is also consistent with the comparatively low 4.5 eV work function for FTO.²¹ Therefore, even in the absence of a secondary interfacial phase, the CGSe/FTO contact is not expected to be optimum for holes’ extraction. We therefore believe at this stage that the difference in J_{sc} between both conditions should be ascribed to a combination of increased bulk recombination and increased series resistance at the CGSe/FTO interface, though both hypotheses will require deeper investigations.

As a conclusion to Figure 2, no appreciable difference exist in terms of voltage when using an Mo interlayer, but J_{sc} and FF are markedly improved yielding a record efficiency of 4.4% without anti-reflective coating (ARC). This observation is consistent with an

FIGURE 2 J-V curves and photovoltaic parameters of samples with different substrates fluorine-doped tin oxide (FTO) and FTO/15 nm Mo



| Sample | Voc [mV] | Jsc [mA/cm ²] | FF [%] | Eff [%] | Rs [Ω.cm ²] | Rsh [Ω.cm ²] | J ₀ [mA/cm ²] | n |
|-------------|----------|---------------------------|--------|---------|-------------------------|--------------------------|--------------------------------------|------|
| FTO | 627 | 10.6 | 49.1 | 3.3 | 4.2 | 487 | 9.70E-06 | 1.94 |
| FTO/15nm Mo | 631 | 13.4 | 52.2 | 4.4 | 15.7 | 2.0E+04 | 2.00E-05 | 1.96 |

improvement of the contact's ohmicity; indeed, the bare FTO sample has a more pronounced crossover between the illuminated and the dark curves, a strong indicator of the presence of a barrier at the back interface. No significant differences are observed in terms of diode quality factor n nor in the reverse saturation current J_0 ; the latter point is specifically ascribed to recombination²² and would necessitate a more thorough analysis with, for example, temperature-dependent characterizations. The ideality factor remaining below 2 indicates that the recombination pathway is dominated by bulk/space charge region recombination rather than being multistep.

Figure 3 displays the external quantum efficiency (EQE) curves of both samples. In the absence of a Mo interlayer, one observes a clear decline in the carrier collection in the low-energy region, which can be ascribed to either back interface recombination (an interpretation previously dismissed) or poor carrier diffusion length, thus a decreasingly efficient carrier collection as electrons are generated further from the p-n junction. This tends to indicate that the Mo interlayer not only does improve the quality of the back interface but also may have a positive influence on the absorber's bulk properties. Hence, whereas series resistance does indeed affect the FF of the devices without Mo interlayer, the lower J_{sc} appears more related to a poor collection of minority carriers due to a low diffusion length rather than relating solely on a resistive effect. When comparing those EQE curves with those reported in Choi *et al.*,⁷ where CGSe grown on a bare ITO and CGSe grown on a Mo electrode without TCO are realized, one can notice an important difference. In our results, the EQE difference depends on the incident energy as previously mentioned, whereas the EQE difference from Choi *et al.*⁷ appears more homogeneously distributed in energy. In the case of our work, a TCO layer is present in

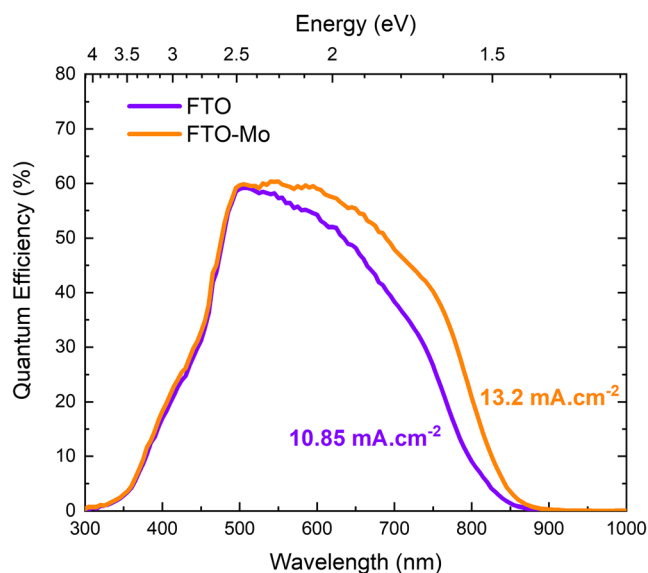


FIGURE 3 Compared normalized external quantum efficiency of samples with different substrates fluorine-doped tin oxide (FTO) and FTO/15 nm Mo

both samples, thus blocking all Na diffusion from the soda lime glass (SLG) substrate.¹³ Therefore, the different observations made in our work compared to the work from Choi *et al.*⁷ are in our opinion likely to be related to a difference in alkali diffusion from the substrate. Future investigations ought to carefully consider this aspect for comparisons to remain relevant.

The bandgap difference between both EQE curves of Figure 3 is evaluated by a Tauc plot and the first derivative method of the EQE, both of which can be found in Supporting Information Figure S2. The difference is found to be 0.03 and 0.04 eV, respectively, which corresponds to a 15 and 19 nm shift in bandgap, depending on the chosen method. Considering an optimistic accuracy of ± 5 nm for the monochromator of the EQE measuring system, this translates into a bandgap difference beyond the error bar of about 5–10 nm. Such difference is far from sufficient to explain the discrepancy in short-circuit current between both samples. It remains nevertheless appreciable and is ascribed to the existence of a Cu-poorer phase with a slightly larger bandgap in the absence of Mo. The homogenization of the Cu distribution in the presence of interfacial Mo is addressed in the following part.

To confirm this hypothesis, further characterization of the two absorbers grown on bare FTO and on FTO/15 nm Mo has been performed by X-ray diffraction (XRD) and Raman scattering measurements. The corresponding patterns of the XRD analysis are shown in Figure 4. Both absorbers present roughly similar diffractograms, an expected result for absorbers of similar overall composition. However, the chalcopyrite peaks from the absorber grown on bare FTO tend to appear at higher angles and have a higher full width at half maximum. In addition to this broadening of the peaks, the peak located in the region between 45.5° and 46° shows an additional contribution in the

form of a shouldering at lower angles. These observations are consistent with the presence of two chalcopyrite phases in the absorber grown on the bare FTO back contacts, being one of these phases characterized by a lower Cu content. This observation confirms the previously made hypothesis regarding the lower homogeneity in Cu distribution for absorbers grown on bare FTO.

The Raman spectra measured from both the front and back surface of the absorbers are shown in Figure 5. The spectra are characterized by an intense peak close to 183 cm^{-1} and several less intense and strongly overlapped peaks. Most of the peaks were assigned to the CGSe chalcopyrite phase and are in accordance with the previous studies.^{23,24} Also, some additional peaks were found at 166 and 199 cm^{-1} . The former peak is attributed to the presence of the ordered vacancy compound (OVC) phase in accordance with Xu *et al.*,²⁵ which is known to be beneficial when forming at the front surface of the chalcopyrite-based solar cells.²⁶ On the other hand, the peak at 199 cm^{-1} was assigned to a detrimental Cu–Au polymorph of the CGSe compound, by analogy with CuInSe_2 compound.²⁴ Finally, in the case of the spectrum measured on the back side of the sample on FTO/Mo substrate, a clear peak of MoSe_2 phase can be observed at 241 cm^{-1} ,²⁷ confirming the selenization of the Mo interlayer. The comparison of Raman spectra of the absorbers grown on bare FTO and FTO/Mo substrate allows to conclude that there is insignificant change in the amount of secondary phases (OVC and Cu–Au

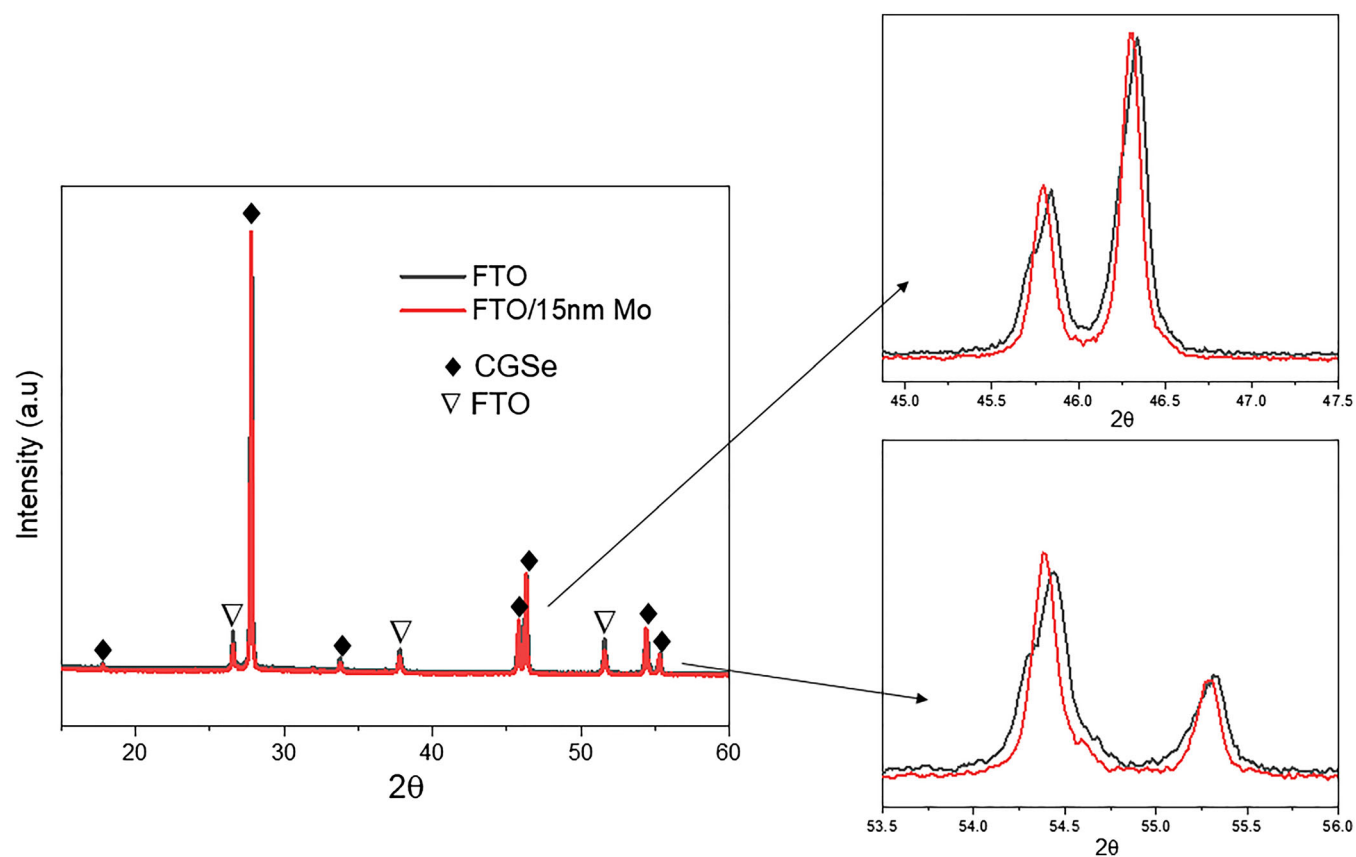
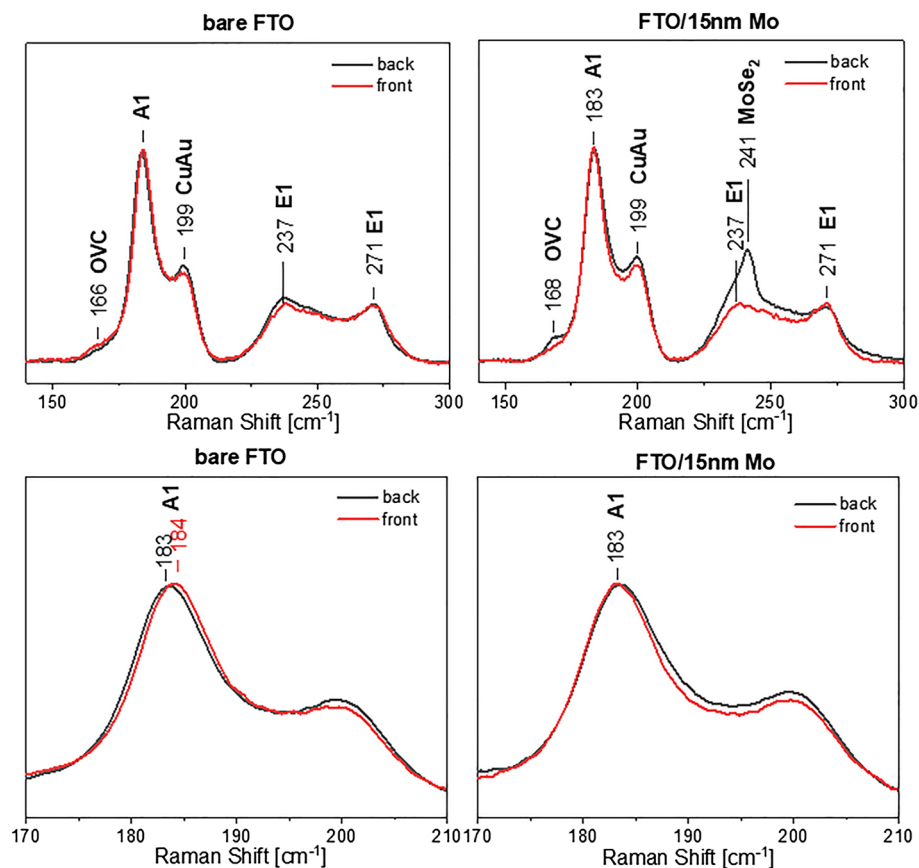


FIGURE 4 XRD diffractograms of samples with different substrates fluorine-doped tin oxide (FTO) and FTO/15 nm Mo

FIGURE 5 Raman spectra with a 532 nm laser of samples with different substrates FTO and FTO/15 nm Mo. The lower panels represent a zoomed range near the main A_1 symmetry peak.



polymorph) in both compounds at the back and front side, and the most evident difference was attributed to the shift of the A_1 symmetry peak assigned to the main chalcopyrite phase. In the case of the bare FTO, a shift of the A_1 mode peak from 183 cm^{-1} at the back to 184 cm^{-1} at the surface can be clearly seen. In the case of familiar CuInSe_2 compounds, the observed shift was attributed to the change of the Cu content inside the chalcopyrite phase,²⁸ meaning a Cu-poor composition of studied CGSe at the surface to more stoichiometric at the back side. This difference in the position of A_1 symmetry peak also correlates with the double structure of some of the reflexes in the XRD diffractograms, confirming the formation of two layers with different Cu content in the absorber deposited on the bare FTO substrate. On the contrary, no shift of the peak can be seen in the spectra measured on the back and front sides of the CGSe deposited on the FTO/Mo substrate, allowing to conclude about higher in-depth homogeneity in Cu distribution of this absorber. This may have a positive effect on the charge carriers' diffusion length and as a result on the observed improvement of short-circuit current.

To summarize on the interplay between CGSe absorbers and TCO back contacts:

- Similar to what is known for the In-containing counterparts, an ultrathin Mo interlayer at the TCO/absorber interface proves to be very beneficial to pure Ga CuGaSe₂-based solar cells, in all likelihood by creating a hole-transporting MoSe₂ layer during the high-temperature treatment phase of the fabrication process.

- The analysis of the EQE curves and the device simulation results indicate that the improvement of the current in the presence of interfacial MoSe₂ is not related to a quenching of back contact recombination as photocarriers should not be able to diffuse that far in the film but is rather mainly due to an improvement of the bulk material transport properties, which raises the question on possible differences existing in the nucleation of CuGaSe₂ on FTO and on Mo/MoSe₂. This is demonstrated by the XRD and Raman analysis showing a clear difference in the bulk of CGSe absorber grown on FTO and FTO/Mo. The lower current density for devices grown on bare FTO back contact could also be partly related to a higher series resistance as shown from the lower FF values and diode fitting. As no secondary phase was detected at the back interface in the Raman analysis, it is likely that the additional hole barrier existing in the case of a bare FTO back contact results from a mismatch in Fermi levels between FTO and CuGaSe₂.

2.2 | Optical properties as top cell in a tandem design

In order to analyze the potential use of the devices as top cells in a tandem architecture, the optical properties of the cells, and particularly their transparency below the bandgap of the absorber, have been measured. The measured optical transmission of the complete stacks with and without interfacial Mo is presented in Figure 6. In the 800–

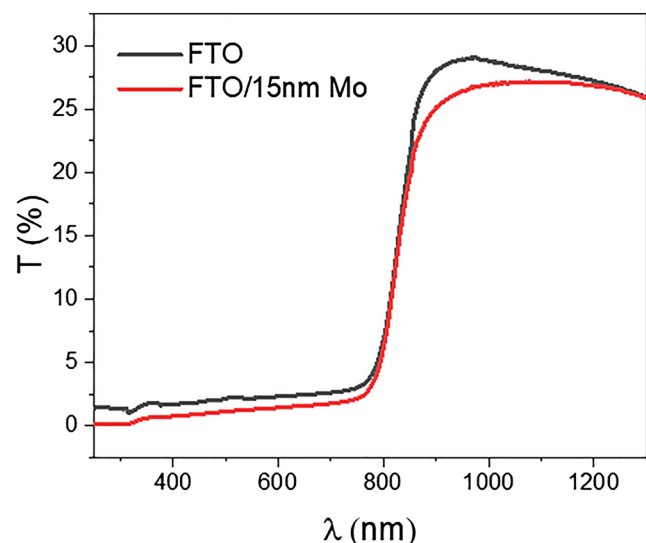


FIGURE 6 Transmission with different substrates fluorine-doped tin oxide (FTO) and FTO/15 nm Mo

1250 nm wavelength range, relevant if considering a ~ 1.0 eV band-gap for the bottom cell, the experimental transmission for CuGaSe_2 on a bare FTO substrate reaches a value of 30% and declines slightly toward 26%. The devices including a Mo interlayer display an almost similar optical transmission, albeit with a slightly lower value of 26% in the 800–1000 nm range.

The current optical transmission falls short to the value needed for a top cell application. One can note the absence of interference fringes in the curves, which is an indication of rough interfaces and light scattering. The optical modeling of an equivalent material stack has been performed using an in-lab developed transfer matrix code running on MatLabTM,²⁹ where light scattering effects can be modeled following a methodology similar to Ogilvy.³⁰ The calculated transmission curves for a material stack, including an ultrathin MoSe_2 interlayer at the FTO/CGSe interface, are presented in Figure 7.

Without considering surface roughness (Figure 7B), clear interference fringes are visible in the simulated transmission, and the overall transmission is in the 50% region below the absorber band-gap. When introducing a 100 nm RMS roughness from the front window to the absorber front interface (Figure 7A), a realistic value considering this type of device, the modeled transmission below the CGSe bandgap falls in the 30%–35% range, whereas interference fringes almost fully disappear. Therefore, it appears that improving the specular properties of front window interfaces is of major importance for the future design of CGSe-based top cells in a tandem design. Methods, such as Br_2 -based etching, have already been proven valuable in that regard for CIGSe,^{31,32} with a final absorber RMS well below 50 nm being achieved. Whereas focusing on improving the PV properties of wide bandgap chalcopyrite is of course an important aspect to design a top cell, the community is also advised to concomitantly tackle the issue of sub-bandgap device optical transparency and target values above 60%.

2.3 | CGSe absorber growth parameters and optimization

In a second part, the influence of several parameters of absorber synthesis was investigated, focusing specifically on the annealing temperature (500°C, 570°C, and 600°C) and pressure conditions (low pressure “LP” at 1.5 mbar under Ar flux or high pressure “HP” 850 mbar in static mode) of the one-step process described in the Section 5 below. Several batches of solar cells were realized, and a representative set of samples is presented here. As the FTO/15 nm Mo back interface was demonstrated to be the most favorable one, all samples reported in the following are fabricated with such back contact.

The figures of merit extracted from the J-V analysis of corresponding solar cells are reported in Figure 8.

The first and most important observation relates to the temperature of the reactive annealing process; indeed, an optimum exists at 570°C, and samples fabricated at 500°C and 600°C do not permit to obtain a PV conversion efficiency above 1%. As seen in the SEM micrographs in Figure 9, a low annealing temperature expectedly leads to a lower crystallinity, whereas conversely, the grain size is increasing within the temperature. Nonetheless, the devices fabricated at 600°C are barely functional in our sample series, which could appear counterintuitive as those samples have the best morphology. The likeliest hypothesis is that temperatures of 600°C and above significantly degrade the FTO back contact/interface. A similar effect has been previously observed in the case of other TCO back contacts (ITO), which showed a detrimental influence on the solar cells' efficiency when the deposition temperatures increased above 600°C due to the appearance of the In–Se amorphous phase at the absorber/back contact interface.¹²

It should moreover be noted that the best results were obtained when annealing in a single step at 570°C low-pressure conditions (1.5 mbar) rather than at high-pressure conditions (500 to 800 mbar, rising with temperature), and multistep annealing processes (not reported here) combining both high-pressure and low-pressure steps did not lead to any gain in performance. In optimized conditions, a PV efficiency in the 3.5%–4.0% range can be consistently obtained, with a very low data spread for the current density and voltage.

The process was repeated in several batches of similar conditions at 570°C and 1.5 mbar and is deemed fairly reproducible. Finally, a champion cell with a conversion efficiency of 5.4% has been obtained, currently the highest value reported for this class of material on transparent substrate (see J-V curve and corresponding EQE of this cell in Figure 10).

3 | STRATEGIES FOR DEVICE OPTIMIZATION

Whereas the present study compiles a set of results allowing to reproducibly obtain wide bandgap CGSe solar cells on transparent substrate with efficiencies at the state-of-the-art level, several challenges remain and should be considered for future investigations.

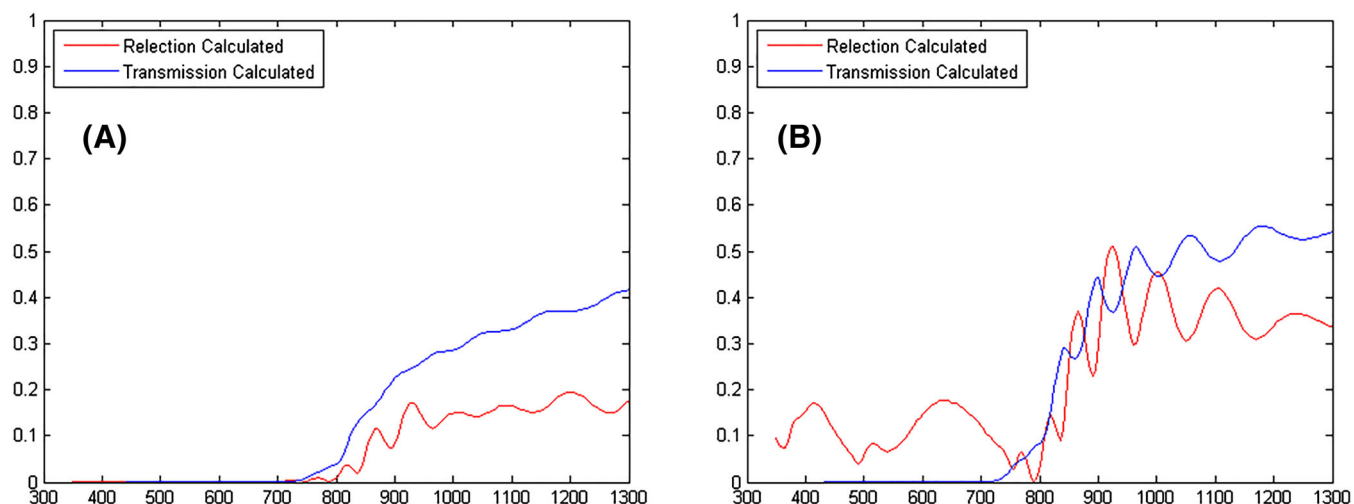
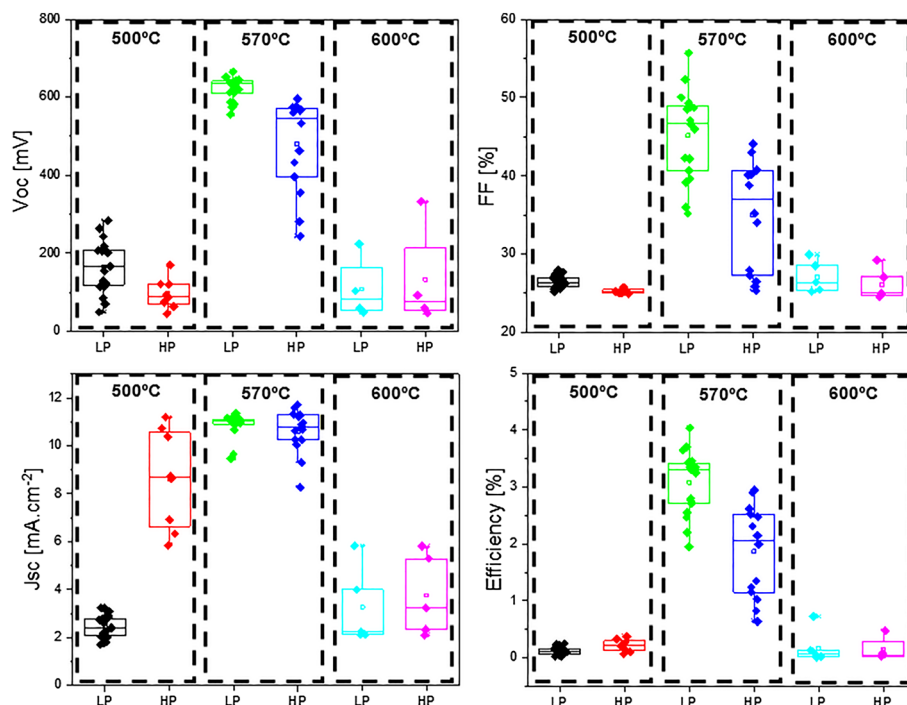


FIGURE 7 Calculated transmission and reflection of an equivalent material stack to the one reported in this work with light scattering effects (A) and with perfectly specular surfaces (B)

FIGURE 8 Photovoltaic parameters of the solar cells prepared with different processes



Firstly, we mostly reported on complete solar cell devices' analysis, and whereas material characterizations of the CGSe films are also presented, the exact interplay between performance, material properties, and growth conditions remain vastly uncharted. It appears that high-temperature annealing of CGSe absorbers may be detrimental to performance, a counterintuitive yet tangible conclusion to the results presented here. Also, the loss mechanisms related to the bare FTO interface compared to the interface including an ultrathin Mo layer require additional work beyond the scope of the present one; whereas various hypotheses are proposed here and are often supported by consistent data, the fact that the highest voltage values remain mostly similar raises unanswered questions regarding the voltage bottleneck.

Nevertheless, a set of stable conditions is presented, including an ultrathin 15 nm Mo interlayer at the back interface, permitting to reproducibly obtain conversion efficiencies above 4.5%, with a record value of 5.4%. Our future work will include an improvement of data homogeneity (metallic grid and improvement of the reactive annealing source geometry) as well as more exhaustive characterizations and methods, such as using mechanical liftoff to accurately characterize the absorber's back interface.

The devices reported here use CdS as buffer layer. It is the most widely used partner layer for chalcopyrite solar cells and can thus be considered a reference in that regard. It is nevertheless not adapted to the wide bandgap compound investigated here from a band alignment

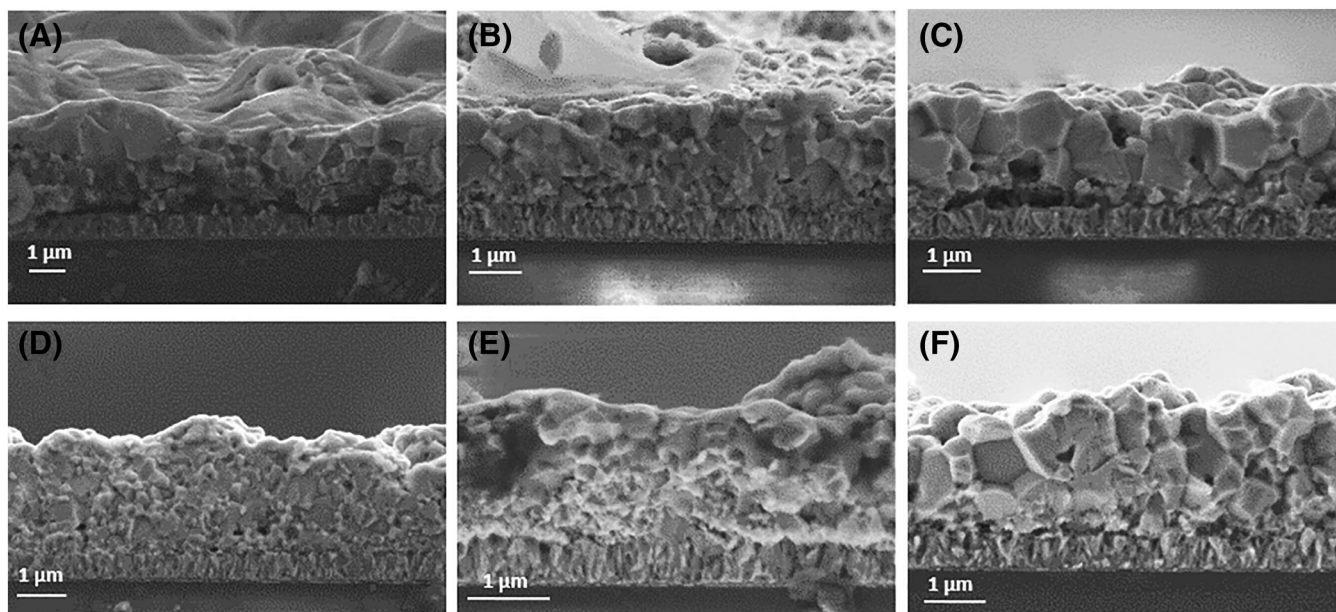


FIGURE 9 SEM images of the solar cells prepared with different processes (A) at 500°C and low pressure 1.5 mbar with Ar flux (B) at 570°C and low pressure 1.5 mbar with Ar flux (C) at 600°C and low pressure 1.5 mbar with Ar flux processes (D) at 500°C and high pressure 800 mbar in static mode (E) at 570°C and high pressure 800 mbar in static mode (F) at 600°C and high pressure 800 mbar in static mode

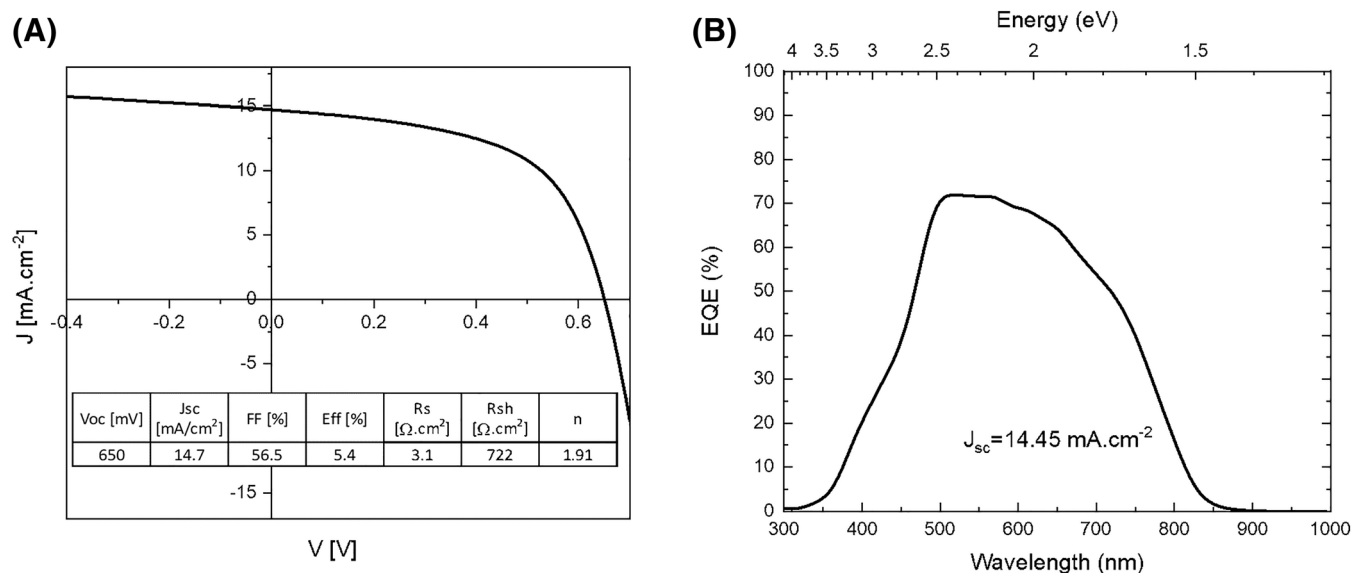


FIGURE 10 (A) J-V curves and photovoltaic parameters of the CuGaSe₂ champion cell with a substrate fluorine-doped tin oxide (FTO)/15 nm Mo. (B) Corresponding external quantum efficiency (EQE) curve

viewpoint and represents a significant source of voltage loss. It is currently our leading hypothesis explaining that devices with and without interfacial Mo reach a similar maximum voltage in record cells. The replacement of CdS by a wider bandgap buffer layer, such as zinc sulphide (ZnS) would additionally, leads to a J_{sc} improvement thanks to an increased absorption in the UV high-energy region. An optical modeling of complete solar stacks comparing CdS and ZnS buffer layers (Figure S3) reveals that the absorption in the CGSe layer using such buffer layer would increase the current by $+1.66 \text{ mA.cm}^{-2}$.

Alkali doping has proven instrumental in the success of narrow bandgap chalcopyrite solar cells, especially with the recent

incorporation of heavy alkali elements following the crystallization of the absorber film.³³ In the presented work, FTO acts as an efficient barrier to the diffusion of sodium from the SLG substrate, and no intentional Na doping was introduced. Preliminary experiments using predeposition of sodium in the layers were not fruitful with the apparition of pinholes in the sample. Future experiments will need to improve on that aspect, not only by investigating predeposition methods for alkali diffusion during growth but also by making use of post-deposition treatments, such as those widely reported for narrow gap CIGS.³⁴

Finally, and whereas improving the PV performance of the devices is of course the main problem to be tackled, the transparency

of the solar cells ought also to be improved for tandem device applications. As discussed in Section 2.2, improving the specular properties of the absorber and the front window is of high importance as an excessive light scattering leads to a decline in the optical transmission of the devices. In addition, we have previously suggested that transition metal oxides, such as MoO_3 , hold more promises to obtain CGSe solar cells highly transparent below the absorber bandgap,²⁹ and experimental methods allowing the realization of such architecture will have to be developed.

Considering the aforementioned limitations and necessary future optimizations, we believe that realizing devices exceeding the 10% efficiency threshold combined with a transparency above 50% below the CGSe bandgap should be seen as a challenging yet achievable target for the community and would give relevancy for the wide bandgap chalcopyrite family of material in the field of tandem solar cells.

4 | CONCLUSION

A route for the fabrication of wide bandgap, pure Ga, CuGaSe_2 -based solar cells on a transparent SLG/FTO substrate is proposed using a combination of metallic precursor sputtering and reactive thermal annealing. The presence of an ultrathin interfacial Mo layer is found essential in improving device performance by not only creating a beneficial MoSe_2 hole transport interlayer but also improving the crystallization and Cu distribution homogeneity, an interpretation consistent by both material and electrical characterization. It was additionally found that reactive annealing temperatures of 600°C markedly degrade the devices' performance, possibly due to a degradation of the FTO substrate. The optimized process was repeated on several batches of samples and appears reproducible. A champion cell efficiency of 5.4% was obtained in optimized conditions, which represents the highest value reported up to now for this material on a transparent electrode substrate. However, the optical transmission of the devices below the absorber bandgap remains in the 30% range, a value deemed insufficient for tandem application. Optical modeling indicates that surface roughness can significantly reduce the optical transmission of the device; thus improving the specular properties of each interface would allow reaching markedly higher optical transmission values up to 60%. Whereas the results of the device efficiency presented here exceed the state of the art for this class of material on transparent substrates, they also offer an overview of its current limitations, and a major research effort from the community will be needed to turn wide bandgap chalcopyrite devices into a credible alternative as top cell in tandem architecture.

5 | EXPERIMENTAL SECTION

5.1 | Solar cells fabrication

The solar cells presented were fabricated with the following material stack: SLG/FTO/(ultrathin Mo)/CGSe/CdS/ZnO/ITO. The SLG/FTO

substrate was purchased from Sigma-Aldrich (reference #735183-5EA). The role of a thin interlayer of Mo (~15 nm nominal) deposited by DC magnetron sputtering is discussed in this article and compared with a precursor deposited directly on the bare FTO. The thickness of the Mo was chosen after optimization of the contact transparency/ohmicity interplay in a process described by Salem *et al.*¹³ The metallic stack of the precursor was also deposited by DC magnetron sputtering in two layers as CuGa/Cu. Using X-ray fluorescence, the final thickness was calibrated to be 760 nm, and the final composition was Cu 44.2%/Ga 55.8%, which is a Cu-poor composition with a ratio Cu/Ga = 0.79. A one-step reactive annealing under Se atmosphere was carried out by placing the metallic precursor in a graphite box with 200 mg of Se powder. The box was inserted in a tubular furnace programed for a one-step annealing with a ramp of 50°C/min until temperatures between 500 and 600°C either with a constant flux of Ar and 1.5 mbar pressure or in a static mode without flux with a pressure varying from 450 to 850 mbar within the temperature during 30 min. The samples were let to naturally cool down at the end of the process. Before depositing the buffer layer, a potassium cyanide (KCN) etching (2%) of 10 min is realized on the absorbers in order to remove potential Cu_xSe_y phases at the surface. The CdS layer was deposited by chemical bath deposition (CBD) at 80°C and the window layer completed by DC sputtering with a 50 nm i:ZnO and a 300 nm ITO layer. Each sample was mechanically scribed with individual solar cells of dimension $3 \times 3 \text{ mm}^2$. Front J-V curves were measured under light conditions using a Sun 3000 class AAA solar simulator (Abet Technologies) calibrated to one sun by using a Si (Newport) reference cell. The EQE spectra of the elaborated solar cells are measured by Bentham PVE300 system calibrated with Si and Ge photodiodes. The fitting of the dark J-V curves was made using a 1-diode model code developed in-lab.

5.2 | Material characterization

The as-deposited CIGSe films and complete solar cells were observed by SEM with a ZEISS Series Auriga microscope using 5 kV accelerating voltage and 5 mm of working distance, to assess their morphology. The morphological features presented in the following section were based on the SEM analysis of hundreds of micrometers (width) in different cross-sectional preparations to avoid biased results. The films were analyzed by XRD using a Bruker D8 Advance, with a scanning rate of $0.6^\circ/\text{min}^{-1}$, a step size of 0.010° , and a 2θ range from 10° to 60° , using the Cu K α radiation (1.5406 Å) operating at 40 kV and 40 mA.

Raman spectroscopy analysis was carried out using a Horiba Jobin-Yvon FHR640 monochromator coupled with the charge-coupled display (CCD) detector. The spectra were measured in back-scattering configuration through a specific probe designed at Institut de Recerca en Energia de Catalunya (IREC). A solid state 532 nm excitation laser was used with the power density below $150 \text{ W}/\text{cm}^2$ to avoid any substantial heating of the samples. The spectra were acquired at six different points of a $1.25 \times 2.5 \text{ cm}^2$ sample at the front and back surfaces of the absorber.

5.3 | Numerical modeling

The electrical simulation of wide bandgap solar cells is performed using SCAPS 3.308, and a set of material parameters were reported elsewhere.²⁹ The optical modeling is made using a self-developed code functioning in MATLAB™ and simulating the complete optical profile of a material stack of known complex optical indices with the transfer matrix approach. Unlike Tiwari *et al.*²⁹ where only the specular component of the light was considered, light scattering effects are taken into account using the Beckmann-Spizzichino method.^{30,35}

ACKNOWLEDGEMENTS

This work is part of the R+D+i Cell2Win project Ref. PID 2019-104372RB-C31 funded by Ministerio de Ciencia e Innovación MCIN/AEI/10.13039/5011000110003. Authors from IREC belong to the SEMS (Solar Energy Materials and Systems) Consolidated Research Group of the “Generalitat de Catalunya” (Ref. 2017 SGR 862). M.P. and M.G. acknowledge the financial support from the Ministerio de Ciencia e Innovación within the Ramón y Cajal (RYC-2017-23758) and Juan de la Cierva (IJC2018-038199-I) programs, respectively.

DATA AVAILABILITY STATEMENT

The data that support the findings of this study are available from the corresponding author upon reasonable request.

ORCID

Angélica Thomere  <https://orcid.org/0000-0002-4686-9778>

REFERENCES

- pv magazine, Module price index, Pv Magazine International (n.d.). Accessed June 21, 2022. <https://www.pv-magazine.com/module-price-index/>
- Nakamura M, Yamaguchi K, Kimoto Y, Yasaki Y, Kato T, Sugimoto H. Cd-Free Cu (In,Ga)(Se,S)₂ thin-film solar cell with record efficiency of 23.35%. *IEEE J Photovolt.* 2019;9:1863-1867. doi:10.1109/JPHOTOV.2019.2937218
- Hanna G, Jasenek A, Rau U, Schock HW. Influence of the Ga-content on the bulk defect densities of Cu (In,Ga)Se₂. *Thin Solid Films.* 2001; 387:71-73. doi:10.1016/S0040-6090(00)01710-7
- Cao Q, Gunawan O, Copel M, et al. Defects in Cu (In,Ga)Se₂ chalcopyrite semiconductors: a comparative study of material properties, defect states, and photovoltaic performance. *Adv Energy Mater.* 2011; 1:845-853. doi:10.1002/aenm.201100344
- Bremner SP, Levy MY, Honsberg CB. Analysis of tandem solar cell efficiencies under AM1.5G spectrum using a rapid flux calculation method. *Prog Photovolt: Res Appl.* 2008;16(3):225-233. doi:10.1002/pip.799
- Larsson F, Nilsson NS, Keller J, et al. Record 1.0 V open-circuit voltage in wide band gap chalcopyrite solar cells. *Prog Photovolt: Res Appl.* 2017;25(9):755-763. doi:10.1002/pip.2914
- Choi JH, Kim K, Eo Y-J, et al. Wide-bandgap CuGaSe₂ thin film solar cell fabrication using ITO back contacts. *Vacuum.* 2015;120:42-46. doi:10.1016/j.vacuum.2015.06.016
- Caballero R, Siebentritt K, Sakurai C, Kaufmann M L-s. CGS-thin films solar cells on transparent back contact. In: *2006 IEEE 4th world conference on photovoltaic energy conference*. Waikoloa, HI: IEEE; 2006:479-482. doi:10.1109/WCPEC.2006.279495
- Schmid M, Caballero R, Klenk R, et al. Experimental verification of optically optimized CuGaSe₂ top cell for improving chalcopyrite tandems. *EPJ Photovolt.* 2010;1:10601. doi:10.1051/epjpv/2010002
- Nakada T, Hirabayashi Y, Tokado T, Ohmori D, Mise T. Novel device structure for Cu (In, Ga) Se₂ thin film solar cells using transparent conducting oxide back and front contacts. *Solar Energy.* 2004;77(6):739-747. doi:10.1016/j.solener.2004.08.010
- Nakada T. Microstructural and diffusion properties of CIGS thin film solar cells fabricated using transparent conducting oxide back contacts. *Thin Solid Films.* 2005;480:419-425. doi:10.1016/j.tsf.2004.11.142
- Fonoll-Rubio R, Placidi M, Hoelscher T, et al. Characterization of the stability of indium tin oxide and functional layers for semitransparent back-contact applications on Cu (In, Ga)Se₂ solar cells. *Solar RRL.* 2022;7:2101071. doi:10.1002/solr.202101071
- Salem MO, Fonoll R, Giraldo S, et al. Over 10% efficient wide bandgap CIGSe solar cells on transparent substrate with Na predeposition treatment. *Solar RRL.* 2020;4(11):2000284. doi:10.1002/solr.202000284
- Orgassa K, Schock HW, Werner JH. Alternative back contact materials for thin film Cu (In,Ga)Se₂ solar cells. *Thin Solid Films.* 2003;431-432:387-391. doi:10.1016/S0040-6090(03)00257-8
- Jehl Li-Kao Z, Naghavi N, Erfurth F, et al. Towards ultrathin copper indium gallium diselenide solar cells: proof of concept study by chemical etching and gold back contact engineering. *Prog Photovolt: Res Appl.* 2012;20(5):582-587. doi:10.1002/pip.2162
- Abou-Ras D, Kostorz G, Bremaud D, et al. Formation and characterization of MoSe₂ for Cu (In,Ga)Se₂ based solar cells. *Thin Solid Films.* 2005;480-481:433-438. doi:10.1016/j.tsf.2004.11.098
- Wada T, Kohara N, Nishiwaki S, Negami T. Characterization of the Cu (In,Ga)Se₂/Mo interface in CIGS solar cells. *Thin Solid Films.* 2001; 387:118-122. doi:10.1016/S0040-6090(00)01846-0
- Simchi H, McCandless BE, Meng T, Shafarman WN. Structure and interface chemistry of MoO₃ back contacts in Cu (In,Ga)Se₂ thin film solar cells. *J Appl Phys.* 2014;115:033514. doi:10.1063/1.4862404
- Yan Y, Li X, Dhare R, et al. SiO₂ as barrier layer for Na out-diffusion from soda-lime glass. In: *2010 35th IEEE photovoltaic specialists conference*. Vol.2010. Honolulu, HI, USA: IEEE; 002519-002521. doi:10.1109/PVSC.2010.5614657
- Paulson PD, Birkmire RW, Shafarman WN. Optical characterization of CuIn_{1-x}Ga_xSe₂ alloy thin films by spectroscopic ellipsometry. *J Appl Phys.* 2003;94(2):879-888. doi:10.1063/1.1581345
- Han D, Wu C, Zhao Y, Chen Y, Xiao L, Zhao Z. Ion implantation-modified fluorine-doped tin oxide by zirconium with continuously tunable work function and its application in perovskite solar cells. *ACS Appl Mater Interfaces.* 2017;9(48):42029-42034. doi:10.1021/acsami.7b12476
- Cuevas A. The recombination parameter J₀. *Energy Procedia.* 2014; 55:53-62. doi:10.1016/j.egypro.2014.08.073
- Ramírez FJ, Rincón C. Polarized micro-Raman spectra in CuGaSe₂. *Solid State Commun.* 1992;84(5):551-556. doi:10.1016/0038-1098(92)90188-F
- Izquierdo-Roca V, Fontané X, Saucedo E, et al. Process monitoring of chalcopyrite photovoltaic technologies by Raman spectroscopy: an application to low cost electrodeposition based processes. *New J Chem.* 2011;35(2):453-460. doi:10.1039/C0NJ00794C
- Xu C-M, Huang W-H, Xu J, et al. Defect-induced structural disorder in tetragonal Cu (In_{1-x}Ga_x)₂Se₈ thin films investigated by Raman spectroscopy: the effect of Ga addition. *J Phys Condens Matter.* 2004; 16(23):4149-4155. doi:10.1088/0953-8984/16/23/029
- Zhang SB, Wei S-H, Zunger A, Katayama-Yoshida H. Defect physics of the CuInSe₂ chalcopyrite semiconductor. *Phys Rev B.* 1998;57(16): 9642-9656. doi:10.1103/PhysRevB.57.9642
- Nam D, Lee J-U, Cheong H. Excitation energy dependent Raman spectrum of MoSe₂. *Sci Rep.* 2015;5(1):17113. doi:10.1038/srep17113

28. Guc M, Bailo E, Fonoll-Rubio R, et al. Evaluation of defect formation in chalcopyrite compounds under Cu-poor conditions by advanced structural and vibrational analyses. *Acta Mater.* 2022;223:117507. doi:[10.1016/j.actamat.2021.117507](https://doi.org/10.1016/j.actamat.2021.117507)
29. Tiwari KJ, Giraldo S, Placidi M, et al. Feasibility of a full chalcopyrite tandem solar cell: a quantitative numerical approach. *Solar RRL.* 2021; 5(7):2100202. doi:[10.1002/solr.202100202](https://doi.org/10.1002/solr.202100202)
30. Ogilvy JA. Wave scattering from rough surfaces. *Rep Prog Phys.* 1987; 50(12):1553-1608. doi:[10.1088/0034-4885/50/12/001](https://doi.org/10.1088/0034-4885/50/12/001)
31. Canava B, Guillemoles JF, Vigneron J, Lincot D, Etcheberry A. Chemical elaboration of well defined Cu (In,Ga)Se₂ surfaces after aqueous oxidation etching. *J Phys Chem Solid.* 2003;64(9-10):1791-1796. doi:[10.1016/S0022-3697\(03\)00201-4](https://doi.org/10.1016/S0022-3697(03)00201-4)
32. Bouttemy M, Tran-Van P, Gerard I, et al. Thinning of CIGS solar cells: part I: chemical processing in acidic bromine solutions. *Thin Solid Films.* 2011;519(21):7207-7211. doi:[10.1016/j.tsf.2010.12.219](https://doi.org/10.1016/j.tsf.2010.12.219)
33. Nakamura M, Yamaguchi K, Kimoto Y, et al. (In,Ga)(Se,S)₂ thin-film solar cell with record efficiency of 23.35%. *IEEE J Photovolt.* 2019; 9(6):1863-1867. doi:[10.1109/JPHOTOV.2019.2937218](https://doi.org/10.1109/JPHOTOV.2019.2937218)
34. Chirilă A, Reinhard P, Pianezzi F, et al. Potassium-induced surface modification of Cu (In,Ga)Se₂ thin films for high-efficiency solar cells. *Nat Mater.* 2013;12(12):1107-1111. doi:[10.1038/nmat3789](https://doi.org/10.1038/nmat3789)
35. Beckmann P., Spizzichino A., The scattering of electromagnetic waves from rough surfaces; 1987. Accessed December 10, 2021. <https://ui.adsabs.harvard.edu/abs/1987ah...book.....B>

SUPPORTING INFORMATION

Additional supporting information can be found online in the Supporting Information section at the end of this article.

How to cite this article: Thomere A, Placidi M, Guc M, et al. 2-step process for 5.4% CuGaSe₂ solar cell using fluorine doped tin oxide transparent back contacts. *Prog Photovolt Res Appl.* 2023;31(5):524-535. doi:[10.1002/pip.3656](https://doi.org/10.1002/pip.3656)